

Proton and Neutron Inclusive Spectra and the Importance of the Single Nucleon-Nucleon Scattering Process

B. D. Anderson, A. R. Baldwin, A. M. Kalenda, R. Madey, and J. W. Watson
Department of Physics, Kent State University, Kent, Ohio 44242

and

C. C. Chang, H. D. Holmgren, R. W. Koontz, and J. R. Wu^(a)
Department of Physics and Astronomy, University of Maryland, College Park, Maryland 20742
 (Received 18 September 1980)

Comparison of inclusive neutron and proton spectra from 90-MeV protons on ^{27}Al , ^{58}Ni , ^{90}Zr , and ^{209}Bi indicate that single nucleon-nucleon scattering dominates the high-energy regions of forward-angle continuum spectra. The ratios of cross sections observed agree with ratios expected for scattering of the incident proton by a bound target nucleon. For ^{27}Al , a plane-wave-impulse-approximation quasifree-scattering calculation fits forward-angle proton and neutron spectra simultaneously with the same normalization.

PACS numbers: 25.40.Eb, 25.40.Cm

The dominant reaction channels for light ions with bombarding energies above 50 MeV excite the continuum rather than discrete nuclear levels.¹⁻⁵ Studies² of inclusive charged-particle spectra from 90-MeV proton bombardments of ^{27}Al , ^{58}Ni , ^{90}Zr , and ^{209}Bi indicate that the total light-charged-particle yields are about twice the total reaction cross sections for the three lighter targets. A large fraction of these yields was found to lie at energies well above the evaporation peaks. Wall and Roos⁶ noted broad peaks in their (p, p') inclusive spectra at an incident energy of 160 MeV which show the signature of "quasifree" scattering from a bound target nucleon; i.e., the peaks move with the same kinematical relation as for free nucleon-nucleon scattering. Cowley *et al.*⁵ and Alexander *et al.*⁷ concluded that at intermediate energies nucleon-nucleon scattering appears to act as a doorway process leading to more complicated scattering mechanisms. Recently, Wu⁸ showed that a simple plane-wave-impulse-approximation (PWIA) calculation can account for the high-energy portion of the proton continuum produced in (p, p') reactions at 62 and 90 MeV. We measured the inclusive (p, n) spectra from 90-MeV protons on the same target nuclei as were used in the 90-MeV inclusive (p, p') studies of Wu, Chang, and Holmgren.² We observe that the (p, n) and (p, p') spectra have the same shapes and angular dependences in the high-energy continuum region. Furthermore, the observation that the ratio of the yields of protons to neutrons in this region is approximately that expected for quasifree scattering provides additional evidence for the importance of the nucleon-nu-

cleon scattering mechanism in proton-induced reactions at incident energies below 100 MeV.

The neutron spectra were measured at the University of Maryland Cyclotron Laboratory with a time-of-flight (TOF) system developed at Kent State University. The high-energy portions of the spectra ($E_n \gtrsim 45$ MeV) were measured with five NE-102 plastic scintillators, each 12.7 cm in diameter by 10.2 cm deep, at flight paths varying from 2 to 5 m. The low-energy portions of the spectra ($E_n \lesssim 45$ MeV) were measured with three NE-213 liquid scintillators, each 5.08 cm in diameter by 5.08 cm deep, at flight paths of 1 m. Pulse-shape discrimination was used to eliminate γ -ray backgrounds in the spectra from the NE-213 detectors; room-scattered backgrounds were measured with iron shadow shields placed halfway between the target and each detector. The neutron detector efficiencies were calculated with an improved version of the Monte Carlo code of Cecil, Anderson, and Madey.⁹ The complete experimental results and procedures will be published in a later paper.

Typical (p, n) spectra at two angles are compared in Fig. 1 with the (p, p') spectra of Wu, Chang, and Holmgren² for ^{27}Al , ^{58}Ni , ^{90}Zr , and ^{209}Bi . Comparisons at other angles show the same features. While the high-energy neutron spectra are similar in shape to the proton spectra for all target nuclei, they differ in the evaporation region. The yields of high-energy neutrons are about one-half of the proton yields. As the target mass increases, the low-energy ($\lesssim 20$ MeV) neutron yields increase compared to the proton yields and exceed the proton yields for

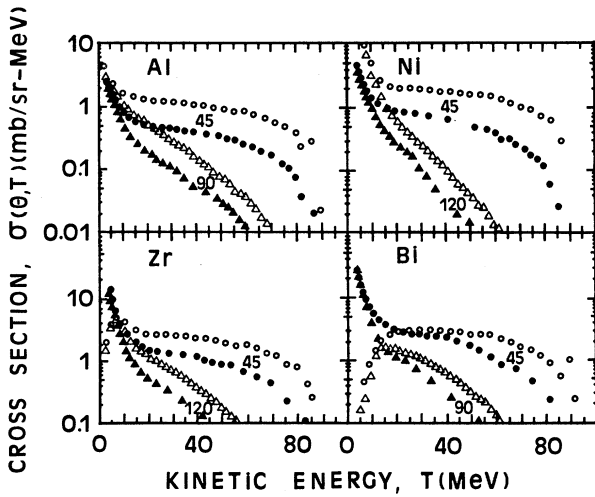


FIG. 1. A comparison of proton (open symbols) and neutron (closed symbols) spectra at 45 and 90 or 120 deg, as indicated, from the bombardment of ^{27}Al , ^{58}Ni , ^{90}Zr , and ^{209}Bi by 90-MeV protons.

the heaviest target (^{209}Bi). These basic characteristics of both the neutron and the proton spectra can be understood qualitatively in terms of the dominance of the one-step quasifree scattering mechanism in the high-energy region with evaporation accounting for low-energy yields.

For single-step quasifree nucleon-nucleon scattering, an incident-proton interaction with a target proton can contribute only to the yield of protons, whereas an incident-proton interaction with a target neutron can contribute to both the proton and the neutron yields. Thus, the ratio of protons to neutrons emitted from a target with N neutrons and Z protons is expected to be approximately

$$\sigma(p, p')/\sigma(p, n) = (Z\sigma_{pp} + N\sigma_{pn})/N\sigma_{pn}, \quad (1)$$

where σ_{pp} and σ_{pn} are effective cross sections for p - p and p - n scattering, respectively, which represent averages over the quasifree scattering angle and energy of the proton and target nucleon. Using the differential cross section at $\theta_{c.m.} = 90^\circ$ and an effective energy of about 120 MeV, we find that this crude expression gives approximately the observed ratios for all four targets: The observed ratios decrease from about 2.5 for ^{27}Al to 1.7 for ^{209}Bi while Eq. (1) gives roughly 2.6 and 2.1, respectively. In contrast, the ratio for equilibrium-type processes would depend on, in addition to the neutron-to-proton ratio, the Q values as well as Coulomb and angular-momentum barriers, and would not be expected to exhibit any simple dependence on Z and N .

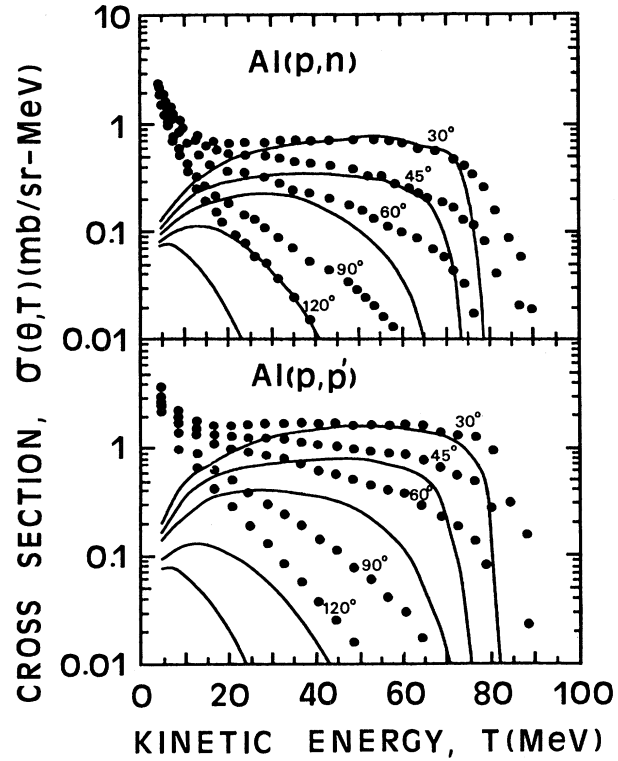


FIG. 2. Comparisons of neutron and proton spectra (solid circles) from the bombardment of an ^{27}Al target by 90-MeV protons with the predictions (solid lines) of a PWIA calculation for quasifree scattering (see text).

In Fig. 2, we compare the $^{27}\text{Al}(p, p')$ and $^{27}\text{Al}(p, n)$ spectra with the PWIA quasifree calculations made with the code of Wu.⁸ These calculations take into account the effects of Fermi motions of the target nucleons and include separate p - p and p - n cross sections taken from experimental measurements,^{10,11} as well as a separate summation over all single-particle states for both target neutrons and protons. The binding energies and potentials for each state were obtained from Elton and Swift.¹² The calculated spectra, which overestimate the experimental yields as expected in PWIA, were normalized to the most forward-angle data by adjusting the number of nucleons participating in the collision from each single-particle state. The calculations use the same normalizations for both the neutron and the proton spectra and were obtained with 60% of the nucleons in the outermost shell and 20% of the nucleons in the inner shells. Although the calculation underestimates the large-angle yield, it agrees to within about $\pm 15\%$ with the high-energy portions of the forward-angle neutron and proton spectra.

Although the normalizations for each target nu-

cleus are arbitrary, the fact that the high-energy portions of both neutron and proton forward-angle spectra are fitted simultaneously by calculations with use of the *same* normalization suggests that the single nucleon-nucleon scattering mechanism accounts for most of the continuum spectrum above the evaporation peaks. The systematic variation of the ratios of neutron to proton yields with N and Z in approximate agreement with Eq. (1) provides additional evidence of the importance of the single nucleon-nucleon scattering mechanism. The combination of these results and the recent particle-particle coincidence studies of reactions induced by 100-MeV protons⁵ demonstrate that the interaction of medium-energy protons with nuclei is dominated by nucleon-nucleon interactions.

The authors wish to express their thanks to N. S. Chant, E. F. Redish, P. G. Roos, and P. C. Tandy for stimulating discussions. This work was supported in part by the National Science Foundation.

^(a)Present address: Bell Laboratories, Chicago, Ill. 60540.

¹F. E. Bertrand and R. W. Peelle, *Phys. Rev. C* **8**, 1045 (1973).

²J. R. Wu, C. C. Chang, and H. D. Holmgren, *Phys. Rev. C* **19**, 698 (1979).

³J. R. Wu, C. C. Chang, and H. D. Holmgren, *Phys. Rev. C* **19**, 370 (1979).

⁴J. R. Wu, C. C. Chang, and H. D. Holmgren, *Phys. Rev. C* **19**, 659 (1979).

⁵A. A. Cowley *et al.*, *Phys. Rev. Lett.* **45**, 1930 (1980); H. D. Holmgren, *Bull. Am. Phys. Soc.* **25**, 600 (1980).

⁶N. S. Wall and P. G. Roos, *Phys. Rev.* **150**, 811 (1966).

⁷Y. Alexander, J. W. Van Orden, E. F. Redish, and S. J. Wallace, *Phys. Rev. Lett.* **44**, 1579 (1980).

⁸J. R. Wu, *Phys. Lett.* **91B**, 169 (1980).

⁹R. Cecil, B. D. Anderson, and R. Madey, *Nucl. Instrum. Methods* **161**, 439 (1979).

¹⁰J. N. Palmieri, A. M. Cormack, N. F. Ramsey, and R. Wilson, *Ann. Phys. (N.Y.)* **5**, 299 (1958).

¹¹W. N. Hess, *Rev. Mod. Phys.* **30**, 368 (1958).

¹²L. R. B. Elton and A. Swift, *Nucl. Phys. A* **94**, 52 (1967).

Resonance Structure of the Antisymmetrized Optical Potential

K. L. Kowalski and A. Picklesimer

Department of Physics, Case Western Reserve University, Cleveland, Ohio 44106

(Received 23 September 1980)

An extension of the unsymmetrized optical-potential formalism for two-fragment elastic scattering is found which fully incorporates the Pauli principle without the use of complicated projection operators. The discrete singularities of this optical potential are shown to be correlated with the physical resonance structure of the scattering amplitude.

PACS numbers: 24.10.Ht, 24.50.+q

A new approach to the problem of incorporating the Pauli principle (PP) into the microscopic theory of the optical potential (OP) for elastic nuclear scattering has appeared recently.¹⁻⁵ The development of Refs. 1-5 differs in several important ways from previous studies of this question.^{6,7} Of particular note is the fact that projection operators which do *not* map the space, \mathcal{H}_Λ , of fully antisymmetrized states into itself are employed in Refs. 1-5. Although these projectors are simpler to work with than those defined on \mathcal{H}_Λ , it is then possible that the identification and physical interpretation of the discrete poles in the OP (as a function of the total energy) might be obscured. In the case of distinguishable particles, such poles of the OP are unambiguously correlated with the resonance structure of the scattering amplitude.⁸ In this Letter we estab-

lish that this correlation also holds for the OP defined as in Ref. 1. Our major results consist in what appears to be a direct and physically transparent generalization of the *original* Feshback formalism⁸ to include the PP which retains the same simplicity and practical applicability characteristic of Ref. 8.

In order to maintain a two-body description of the elastic two-fragment scattering, the antisymmetrized transition and OP operators, $T(\hat{\beta})$ and $U(\hat{\beta})$, respectively, are related by¹

$$U(\hat{\beta}) = T(\hat{\beta}) - U(\hat{\beta})P_\beta G_\beta T(\hat{\beta}), \quad (1a)$$

$$= T(\hat{\beta}) - T(\hat{\beta})P_\beta G_\beta U(\hat{\beta}), \quad (1b)$$

where (1b) follows from (1a) if the solution of (1a) is unique. Here β refers to an arbitrary (but fixed) choice of the assignment of identical nucle-